11th International Symposium on Turbulence and Shear Flow Phenomena (TSFP11)
Southampton, UK, July 30 to August 2, 2019

A ONE EQUATION EXPLICIT ALGEBRAIC SUBGRID-SCALE STRESS MODEL

S. Hickel, A. K. Gnanasundaram and T. Pestana
Faculty of Aerospace Engineering
Delft University of Technology
Kluyverweg 1, 2629HS Delft, The Netherlands
s.hickel@tudelft.nl

ABSTRACT

Nonlinear Explicit Algebraic Subgrid-scale Stress Models (EASSMs) have shown high potential for Large Eddy Simulation (LES) of challenging turbulent flows on coarse meshes. A simplifying assumption made to enable the purely algebraic nature of the model is that the Subgrid-Scale (SGS) kinetic energy production and dissipation are in balance, i.e., $\mathcal{P}/\varepsilon = 1$. In this work, we propose an improved EASSM design that does not involve this pre-calibration and retains the ratio $\mathcal{P}/\varepsilon$ as a space and time dependent variable. Our model is based on the partial differential evolution equation for the SGS kinetic energy k_{sgs} and the assumption that the ratio $\mathcal{P}/\varepsilon$ evolves slower in time than k_{sgs}. Computational results for simple cases of forced isotropic turbulence show that the new model is able to track the evolution of the SGS kinetic energy significantly better than the dynamic and non-dynamic EASSMs of Marstorp *et al.* (2009). Also the predicted kinetic energy spectra and resolved dissipation evolution are in excellent agreement with reference data from Direct Numerical Simulations (DNS).

INTRODUCTION AND MOTIVATION

Large Eddy Simulations (LES) is based on filtering the scales of motion in such a way that the energetic scales are resolvable on a reasonably coarse mesh. This introduces an extra unknown into the governing equations, the subgrid-scale (SGS) stress tensor. Not surprisingly, the accuracy of the LES depends on the ability of the models to represent effects of the SGS stresses on the resolved scales of motion.

Eddy viscosity models, such as the dynamic Smagorinsky model (Germano *et al.*, 1991) assume that the SGS stress is linearly proportional to the resolved strain-rate tensor, in a fashion similar to the Boussinesq approximation employed in Reynolds Averaged Navier-Stokes (RANS) simulations. While this assumption offers simplicity and considerable numerical robustness, it is, strictly speaking, invalid even for simple canonical cases such as homogeneous isotropic turbulence (Tao *et al.*, 2000, Horiuti, 2003). A typical approach to improve on this shortcoming is to include a second non-linear tensor in addition to the strain-rate tensor, see Meneveau & Katz (2000) and Wang & Bergstrom (2005), e.g..

More advanced, Nonlinear Explicit Algebraic Subgrid-scale Stress Models (EASSMs) have lately demonstrated very promising results for complex flow scenarios. Marstorp *et al.* (2009) introduced the first EASSM for LES by extending modeling strategies common in Explicit Algebraic Reynolds Stress Models (EARSM, see Taulbee (1992), Girimaji (1996), and Wallin & Johansson (2000), e.g.). Their dynamic and non-dynamic EASSM variants are computationally efficient and outperform classical eddy viscosity models in particular on coarser grids (Montecchia *et al.*, 2017). The improvement in results are primarily attributed to a better representation of the SGS anisotropy.

The general procedure to derive an EASSM for LES is in close analogy to EARSM for RANS. Starting from an evolution equation for the SGS stress tensor, a weak-equilibrium assumption (Rodi, 1972) is employed to eliminate the material time derivative of the SGS anisotropy stress tensor. With the help of the tensorial bases formulation of Pope (1975) for expressing the SGS stress anisotropy and additional models for the remaining terms, such as the pressure-strain correlation and the dissipation tensor, an explicit algebraic relation for the SGS stress tensor is derived. This relation, however, is inherently implicit and non-linear in terms of the SGS stresses, a known difficulty in the world of EARSM. To remove this non-linearity, Marstorp *et al.* (2009) further make the assumption that the SGS turbulent kinetic production $\mathcal{P}$ and the energy dissipation rate ε are in balance.

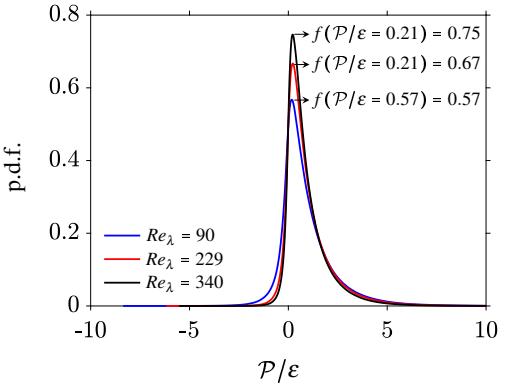

Figure 1: Probability density function of the ratio of subgrid-scale kinetic energy production to dissipation $\mathcal{P}/\varepsilon$ for homogeneous isotropic turbulence different Taylor micro-scale Reynolds numbers (Gnanasundaram *et al.*, 2019).

From a standpoint of mathematical complexity, this perfect equilibrium assumption, i.e., $\mathcal{P}/\varepsilon = 1$, sets the framework for an attractive class of fully explicit and algebraic nonlinear models. Nevertheless, it needs to be pointed out that this assumption significantly limits the generality of the model. Choosing $\mathcal{P}/\varepsilon = 1$ implies that k_{sgs} is globally conserved and its local evolution is purely driven by advection and diffusion. To determine the evolution of k_{sgs}, Marstorp *et al.* (2009) thus used algebraic closures that adapt k_{sgs} instantaneously to the resolved scales. A consequence of this procedure is that such models are unable to accurately capture the temporal evolution of k_{sgs}, which is important in non-equilibrium flows, such as laminar-turbulent transition or adverse pressure-gradient boundary layers.

To emphasize the importance of this point, we show the probability density function (p.d.f.) of the ratio of subgrid-scale kinetic energy production to dissipation, $\mathcal{P}/\varepsilon$, for three different Taylor micro-scale Reynolds numbers $Re_\lambda = 90$, 229 and 340 in Fig. 1. We observe that the p.d.f. is highly skewed and becomes less flat with increasing Re_λ. In all three cases, values significantly smaller than 1 are associated with the maximum probability; we measured $\mathcal{P}/\varepsilon = 0.21$ for $Re_\lambda = 340$ and $Re_\lambda = 229$. This indicates a strong local (in space and in time) imbalance between $\mathcal{P}$ and ε, which should be accounted for in SGS modeling.

Equilibrium of SGS production and dissipation can be assumed only in a statistical sense for the mean quantities in fully developed statistically stationary flows, that is, it may be justified to assume $\langle\mathcal{P}\rangle/\langle\varepsilon\rangle \approx 1$, where $\langle\cdot\rangle$ represents (space, time, or ensemble) averaged quantities. However, this is fundamentally different from $\langle\mathcal{P}/\varepsilon\rangle$ or requiring $\mathcal{P}/\varepsilon$-equilibrium locally and instantaneously. Nevertheless, we should note that the assumption of $\mathcal{P}/\varepsilon = 1$ is not unique to the EASSMs of Marstorp *et al.* (2009), but in fact is implied by linear eddy viscosity models and consequently rather common in SGS modeling.

In this work, we propose and evaluate an alternative modeling approach where $\mathcal{P}/\varepsilon$ is not strictly fixed to unity but can vary arbitrarily in space. While additional closure relations based on similar assumptions are common in the context of EARSM for RANS (see Wallin & Johansson (2000), for example), EASSM for LES that solve for the SGS production-dissipation imbalance are rather unexplored. In the following we propose an alternative way to treat local SGS imbalance effects efficiently in LES.

A NON-EQUILIBRIUM EXPLICIT ALGEBRAIC SUBGRID-SCALE STRESS MODEL

Definitions

Let us first introduce some notations. We are interested in modelling the SGS stress tensor τ_{ij} that appears in the filtered incompressible Navier-Stokes equations:

$$\frac{\partial \widetilde{u_i}}{\partial x_i} = 0 \tag{1}$$

$$\frac{\partial \widetilde{u_i}}{\partial t} + \widetilde{u_j}\frac{\partial \widetilde{u_i}}{\partial x_j} = -\frac{1}{\rho}\frac{\partial \widetilde{p}}{\partial x_i} + \nu\frac{\partial^2 \widetilde{u_i}}{\partial x_i^2} + \frac{\partial \tau_{ij}}{\partial x_j} + f_i\,, \tag{2}$$

where u_i is the velocity component, p is the pressure, ρ and ν are the fluid's density and kinematic viscosity, and f_i is an external body force. The filtering operation is denoted by $\widetilde{(\cdot)}$, and subscript indices are used to represent vectorial and tensorial quantities, where summation over repeated indices is implied.

The SGS terms that result from the filtering procedure that can be expressed using generalized central moments (Germano, 1992). Given three quantities, say α_1, α_2 and α_3, the second-order moments are $\mathcal{G}(\alpha_1,\alpha_2) = \widetilde{\alpha_1\alpha_2} - \widetilde{\alpha}_1\widetilde{\alpha}_2$ and the third-order moments are $\mathcal{G}(\alpha_1,\alpha_2,\alpha_3) = \widetilde{\alpha_1\alpha_2\alpha_3} - \widetilde{\alpha}_1\mathcal{G}(\alpha_2,\alpha_3) - \widetilde{\alpha}_2\mathcal{G}(\alpha_3,\alpha_1) - \widetilde{\alpha}_3\mathcal{G}(\alpha_1,\alpha_2) - \widetilde{\alpha}_1\widetilde{\alpha}_2\widetilde{\alpha}_3$.

Following this notation, we define the SGS stress tensor τ_{ij}, the SGS kinetic energy k_{sgs} and the normalised SGS stress anisotropy a_{ij} as $\tau_{ij} = \mathcal{G}(u_i,u_j) = \widetilde{u_iu_j} - \widetilde{u}_i\widetilde{u}_j$, $k_{sgs} = \frac{1}{2}\mathcal{G}(u_i,u_i) = \frac{1}{2}(\widetilde{u_iu_i} - \widetilde{u}_i\widetilde{u}_i)$ and $a_{ij} = \tau_{ij}/k_{sgs} - (2/3)\delta_{ij}$, where δ_{ij} is the Kronecker delta.

In the absence of any external body force, the evolution equation for the SGS stress tensor τ_{ij} is

$$\frac{D\tau_{ij}}{Dt} + \frac{\partial}{\partial x_k}\Bigg[\underbrace{\mathcal{G}(u_i,u_j,u_k)}_{\text{turbulent transport}} + \underbrace{\frac{1}{\rho}\mathcal{G}(p,u_j)\,\delta_{ik} + \frac{1}{\rho}\mathcal{G}(p,u_i)\,\delta_{jk}}_{\text{pressure transport}} - \underbrace{\nu\frac{\partial\mathcal{G}(u_i,u_j)}{\partial x_k}}_{\text{viscous diffusion}}\Bigg] = \underbrace{-\mathcal{G}(u_j,u_k)\frac{\partial\widetilde{u_i}}{\partial x_k} - \mathcal{G}(u_i,u_k)\frac{\partial\widetilde{u_j}}{\partial x_k}}_{\text{production}} + \underbrace{\mathcal{G}\left(\frac{p}{\rho},\frac{\partial u_j}{\partial x_i}\right) + \mathcal{G}\left(\frac{p}{\rho},\frac{\partial u_i}{\partial x_j}\right)}_{\text{pressure-strain}} \underbrace{-2\nu\mathcal{G}\left(\frac{\partial u_i}{\partial x_k},\frac{\partial u_j}{\partial x_k}\right)}_{\text{dissipation}}, \tag{3}$$

where $D(\cdot)/Dt$ is the material derivative, and the SGS kinetic energy evolution equation

$$\frac{Dk_{sgs}}{Dt} + \frac{\partial\mathcal{T}_k}{\partial x_k} = \mathcal{P} - \varepsilon. \tag{4}$$

is obtained by taking half of the trace of Eq. (3), where $\mathcal{T}_k = \frac{1}{2}\mathcal{T}_{iik}$ is the transport term that combines pressure, turbulent, and viscous effects.

From Eq. (4), we see that the term $(\mathcal{P}-\varepsilon)$ on the right-hand-side (r.h.s.) drives the evolution of the volume averaged k_{sgs}. The transport term $\mathcal{T}_k$ is a transfer term and vanishes when the volume average of Eq. (4) is considered. Therefore, to capture the dynamics of k_{sgs}, the imbalance between $\mathcal{P}$ and ε must be considered.

Equation (3) provides the starting point for the derivation of any EASSM. For simplicity, we reduce Eq. (3) to a compact form, which captures the functional equivalence of the different terms involved:

$$\frac{D\tau_{ij}}{Dt} + \frac{\partial\mathcal{T}_{ijk}}{\partial x_k} = \mathcal{P}_{ij} + \Pi_{ij} - \varepsilon_{ij} \tag{5}$$

The transport term $\mathcal{T}_{ijk}$ includes the turbulent, pressure, and viscous effects present in Eq. (3). The terms on the r.h.s. of Eq. (5), i.e., $\mathcal{P}_{ij}$, Π_{ij}, and ε_{ij} are the SGS kinetic energy

production, the pressure-strain correlation, and the dissipation tensors, respectively. Finding an algebraic relation for τ_{ij} in Eq. (5) requires neglecting the temporal and spatial derivatives on the left-hand-side (l.h.s.) of Eq. (5). To this end, the first term on the l.h.s. of Eq. (5) can be rewritten in terms of the material derivative of the normalized SGS stress anisotropy and the SGS kinetic energy to yield

$$\frac{D\tau_{ij}}{Dt} = k_{sgs}\frac{Da_{ij}}{Dt} + \frac{\tau_{ij}}{k_{sgs}}\frac{Dk_{sgs}}{Dt}. \tag{6}$$

Until this point, no assumptions or simplifications has been made. The first simplification comes from the weak equilibrium assumption, which is borrowed from RANS Reynolds stress models (Rodi, 1972).

Within the context of LES, our interpretation of the weak equilibrium assumption is that a_{ij} in Eq. (6) adjusts so quickly to the local environment defined by the resolved quantities that its material time derivative can be ignored. Thus, the evolution of τ_{ij} is gouverned by the slower evolution of k_{sgs}:

$$\frac{D\tau_{ij}}{Dt} \approx \frac{\tau_{ij}}{k_{sgs}}\frac{Dk_{sgs}}{Dt}. \tag{7}$$

Combining the evolution equation of k_{sgs} (Eq. (4)), and Eq. (5), we obtain

$$\frac{\tau_{ij}}{k_{sgs}}\left(\mathcal{P} - \varepsilon - \frac{\partial \mathcal{T}_k}{\partial x_k}\right) + \frac{\partial \mathcal{T}_{ijk}}{\partial x_k} = \mathcal{P}_{ij} + \Pi_{ij} - \varepsilon_{ij}. \tag{8}$$

After having simplified the first term on the l.h.s. of Eq. (5), the second term is modeled as

$$\frac{\partial \mathcal{T}_{ijk}}{\partial x_k} \propto \frac{\tau_{ij}}{k_{sgs}}\frac{\partial \mathcal{T}k}{\partial x_k}. \tag{9}$$

Similar to the interpretation of the weak equilibrium assumption, where the evolution of τ_{ij} is captured through the evolution of k_{sgs}, Eq. (7), the aforementioned simplification can be viewed in the way that one can forgo computing the transport quantities in the SGS stress evolution equation provided that it is accounted for in the evolution of SGS kinetic energy. This leads us to

$$\frac{\tau_{ij}}{k_{sgs}}\left(\mathcal{P} - \varepsilon\right) = \left(\mathcal{P}_{ij} + \Pi_{ij} - \varepsilon_{ij}\right). \tag{10}$$

The presence of τ_{ij} and $\mathcal{P}$ on the l.h.s. of Eq. (10) gives rise to a nonlinearity in terms of τ_{ij}, because $\mathcal{P} = -\tau_{ij}\widetilde{S}_{ij}$, where $\widetilde{S}_{ij} = (\widetilde{u}_{i,j} + \widetilde{u}_{j,i})/2$ is the resolved strain rate tensor. Marstorp *et al.* (2009) circumvent this difficulty by assuming $\mathcal{P}/\varepsilon = 1$, which removes the non-linearity and the l.h.s. vanishes completely.

Instead of assuming $\mathcal{P}/\varepsilon = 1$, we adopt the methodology commonly seen in RANS (Girimaji, 1996, Wallin & Johansson, 2000), and retain $\mathcal{P}/\varepsilon$ as an extra unknown in the equations. We will revisit the treatment of this ratio at the end of this section. On the r.h.s. of Eq. (10), $\mathcal{P}_{ij}$ is expressed in terms of the anisotropy tensor a_{ij}, rotation rate tensor $\widetilde{\Omega}_{ij} = (\widetilde{u}_{i,j} - \widetilde{u}_{j,i})/2$ and strain rate tensor $\widetilde{S}_{ij}$ as

$$\mathcal{P}_{ij} = k_{sgs}\left[-\frac{4}{3}\widetilde{S}_{ij} - \left(a_{ik}\widetilde{S}_{kj} + \widetilde{S}_{ik}a_{kj}\right) + \left(a_{ik}\widetilde{\Omega}_{kj} - \widetilde{\Omega}_{ik}a_{kj}\right)\right], \tag{11}$$

without loss of generality, whereas Π_{ij} and ε_{ij} require additional models.

For the modeling of the pressure-strain correlation, Π_{ij}, we use the LRR-QI model of Launder *et al.* (1975) with the same constants and coefficients as proposed for RANS. It must be noted that the model for Π_{ij} is not decoupled from ε_{ij}. To understand this, one must look deeper into how the model is constructed. The final expression for the LRR-QI model stems from the separation of the models for the slow and rapid effects of the pressure-strain term in RANS. The joint model for Π_{ij} acts in a way that the slow and rapid pressure-strain tensors decrease the anisotropy of ε_{ij} and $\mathcal{P}_{ij}$, respectively. Based on that, the common practice in RANS is to model the deviator of the dissipation tensor together with the slow pressure-strain term (see Girimaji (1996), Lumley & Newman (1977), e.g.). So, the LRR-QI is a model for $\Pi_{ij} - (\varepsilon^d_{ij} + \varepsilon^s_{ij})$, which can be expressed as

$$\begin{aligned}\Pi_{ij} - (\varepsilon^d_{ij} + \varepsilon^s_{ij}) = &-C_R\varepsilon a_{ij} + \frac{4}{5}k_{sgs}\widetilde{S}_{ij} + \\ &\frac{3}{11}(2+3C_2)k_{sgs}\left(\widetilde{S}_{ik}a_{kj} + a_{ik}\widetilde{S}_{kj} - \frac{2}{3}\widetilde{S}_{kl}a_{kl}\delta_{ij}\right) + \\ &\frac{1}{11}(10-7C_2)k_{sgs}\left(\widetilde{\Omega}_{ik}a_{kj} - a_{ik}\widetilde{\Omega}_{kj}\right) - \frac{2}{3}\varepsilon\delta_{ij}.\end{aligned} \tag{12}$$

The first term on the r.h.s. of Eq. (12) models the slow pressure-strain term, which includes now also the model for ε^d. $C_R = 1.5$ is the Rotta constant and $C_2 = 0.4$. The last term on the r.h.s. is ε^s_{ij} and the rest of the terms provide the model for the rapid pressure-strain term. Combining Eqs. (10) to (12), we can rewrite Eq. (10) as

$$\begin{aligned}\left(a_{ij} + \frac{2}{3}\delta_{ij}\right)\left(\frac{\mathcal{P}}{\varepsilon} - 1\right) = \frac{1}{\varepsilon}\Bigg[&-C_R a_{ij} - \frac{8}{15}k_{sgs}\widetilde{S}_{ij} \\ &+ \left(\frac{9C_2 - 5}{11}\right)\left(\widetilde{S}_{ik}a_{kj} + a_{ik}\widetilde{S}_{kj}\right)k_{sgs} \\ &- \left(\frac{18C_2 + 12}{33}\right)k_{sgs}\widetilde{S}_{kl}a_{kl}\delta_{ij} \\ &+ \left(\frac{1 - 7C_2}{11}\right)\left(a_{ik}\widetilde{\Omega}_{kj} - \widetilde{\Omega}_{ik}a_{kj}\right)k_{sgs} - \frac{2}{3}\varepsilon\delta_{ij}\Bigg].\end{aligned} \tag{13}$$

Explicit relations for a_{ij} can be found from Eq. (13) by substituting the tensorial basis representation of Pope (1975) for a_{ij}. We restrict ourselves to the same ansatz as Marstorp *et al.* (2009), i.e., $a_{ij} = G_1 T^1_{ij} + G_2 T^2_{ij}$, where $T^1_{ij} = \widetilde{S}^*_{ij}$ and $T^2_{ij} = \widetilde{S}^*_{ik}\widetilde{\Omega}^*_{kj} - \widetilde{\Omega}^*_{ik}\widetilde{S}^*_{kj}$, and G_1 and G_2 are functions that must be determined. The superscript $(\cdot)^*$ denotes quantities non-dimensionalized with the timescale $t^* = k_{sgs}/\varepsilon$, that is , $\widetilde{S}^*_{ij} = t^*\widetilde{S}_{ij}$ and $\widetilde{\Omega}^*_{ij} = t^*\widetilde{\Omega}_{ij}$.

Note that the tensorial expansion of a_{ij} in terms of the tensors T^1_{ij} and T^2_{ij} is again borrowed from RANS. In the EARSM of Wallin & Johansson (2000), the use of two tensors to form the basis for a_{ij} is justified in the limit of two dimensional mean flows, where more complex tensors in

the original formulation of Pope (1975) become linearly dependent or zero. This argument is generally not valid for LES as we deal with inherently unsteady three-dimensional velocity fields and other tensors may contribute as well. This should be explored in future work.

The constants G_1 and G_2 can be derived by substituting $a_{ij} = G_1 T^1_{ij} + G_2 T^2_{ij}$ into Eq. (13). Although we selected the same basis tensors as Marstorp *et al.* (2009), our model definitions lead to different functionals for G_1 and G_2:

$$G_1 = -\frac{18}{15}\left[\frac{\left(\frac{9\eta}{4}\right)}{\left(\frac{9\eta}{4}\right)^2 - 2\widetilde{\Omega}^*_{ij}\widetilde{\Omega}^*_{ji}}\right],$$
$$G_2 = \frac{4}{9\eta}G_1\,, \tag{14}$$

where

$$\eta = \frac{\mathcal{P}}{\varepsilon} - 1 + C_R \tag{15}$$

includes the ratio $\mathcal{P}/\varepsilon$, which was retained as an extra unknown.

In order to close the model, we must determine k_{sgs}, ε and $\mathcal{P}/\varepsilon$. For k_{sgs}, we follow Yoshizawa & Horiuti (1985) and use a modeled version of Eq. (4),

$$\frac{Dk_{sgs}}{Dt} - \frac{\partial}{\partial x_j}\left[(\nu_k + \nu)\frac{\partial k_{sgs}}{\partial x_j}\right] = -\tau_{ij}\frac{\partial \widetilde{u}_i}{\partial x_j} - C_c\frac{k_{sgs}^{3/2}}{\ell_{sgs}}\,, \tag{16}$$

where ℓ_{sgs} is the SGS length scale taken as the grid size, $\nu_k = C_k \ell_{sgs}\sqrt{k_{sgs}}$ is an eddy viscosity and the dissipation is modeled as $\varepsilon = C_c k_{sgs}^{3/2}/\ell_{sgs}$. The constants C_c and C_k must be calibrated, which is the topic of the next section.

Finally, we return to the treatment of $\mathcal{P}/\varepsilon$. Instead of formulating additional closure expressions as done in RANS, we propose an approach that uses the fact that we resolve instantaneous quantities in LES. The ratio, $\mathcal{P}/\varepsilon$ can be viewed as a measure for the deviation from the perfect local equilibrium. Any imbalance in this local equilibrium will add or remove kinetic energy to or from the SGS. We assume that this imbalance evolves slowly in time, and propose to take the value of $\mathcal{P}/\varepsilon$ from the previous time step. This simple approach does not impose additional restrictions on the spatial variation of the $\mathcal{P}/\varepsilon$ and does not add to the total number of closure relations needed to solve τ_{ij}.

Because this alternative formulation of the EASSM does not rest on the perfect local equilibrium assumption between $\mathcal{P}$ and ε, we refer to it as the non-equilibrium explicit algebraic (NEA) model. This is not to confused with the weak equilibrium assumption, which is still used to derive the model.

Calibration

The next natural step is to determine the constants C_R, C_k and C_c, in Eqs. (15) and (16). For the two first constants, we use the standard values $C_R = 1.5$ and $C_k = 0.1$ (Rotta, 1951, Yoshizawa & Horiuti, 1985). To calibrate C_c, we consider a reference DNS solution for a case of forced homogeneous turbulence. This reference solution correspond to a fully developed turbulence flow with $Re_\lambda = 220$ in a triply periodic box of size 2π. The DNS is performed with a dealiased pseudo-spectral scheme (Pestana & Hickel, 2019) with 768^3 degrees of freedom. The LES runs are performed with a staggered second-order finite-volume scheme on a 32^3 spatial grid and with a third-order Runge-Kutta scheme in time.

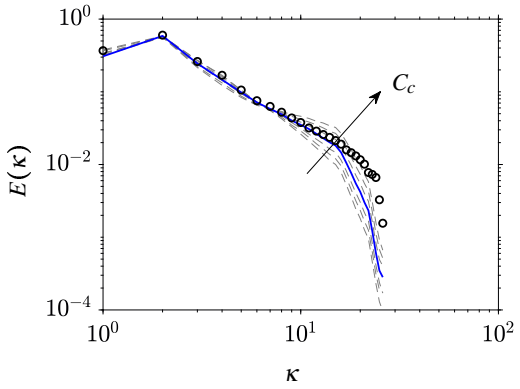

Figure 2: The variation in the time averaged resolved spectrum with C_c; The solid line corresponds to $C_c = 1.55$ and symbols indicate the filtered and time-averaged DNS spectrum.

DNS and LES are initialized with zero velocity and use the forcing scheme of Alvelius (1999) with the same forcing parameters. The force field has a Gaussian spectrum and is designed in such a way that the box-averaged energy input rate $\varepsilon_I = \langle f_i f_i \rangle/2$ is independent of the velocity-force correlation. Instead, it depends solely on the force-force correlation, which is chosen to be statistically the same in both simulations. To compare both the DNS and the LES results, we filter the DNS fields with a box-filter.

Figure 2 shows the three-dimensional spherically averaged energy spectrum for the the DNS and for several LES with different values for $C_c > 1$. It is clear that the model is highly sensitive on the value of C_c. We observe that high values of C_c increase the SGS dissipation ε, but it does not lead to a more dissipative model. In contrast, it has the opposite effect on the large scales: a higher ε reduces the SGS kinetic energy k_{sgs} and hence less energy is drained from the resolved scales. The exact amount of energy drained from the resolved scales ultimately depends on how well the SGS kinetic energy production is modeled. In our formulation, the modeling is such that $\mathcal{P} = k_{sgs} t^* G_1 \widetilde{S}^*_{ij}$; note that T^2_{ij} does not contribute to $\mathcal{P}$. An increased level of ε leads to a slower growth of k_{sgs}, and also lowers t^* as they are inversely related. As a results, the modelled $\mathcal{P}$ reduces and the model in turn drains less energy from the resolved scales. We also clearly see this trend in Fig. 2 where the energy density of the resolved wave numbers increases due to insufficient model dissipation with increase in C_c. We find that the energy spectrum of the DNS in Fig. 2 is best reproduced by the LES with $C_c = 1.55$.

Validation

In this section we test the present model for a case of forced homogeneous turbulence with $Re_\lambda = 340$. Again, DNS simulations are performed to produce a reference solution. For comparison, we also perform LES calculations using the models of Marstorp *et al.* (2009), which are hereafter referred to as the SEA (standard version) and the DEA

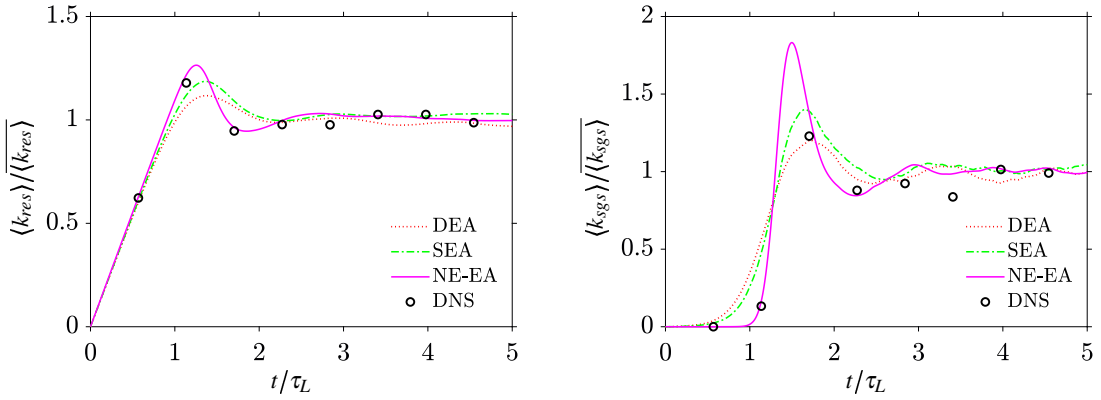

Figure 3: Evolution of the volume averaged resolved kinetic energy (left) and SGS kinetic energy (right).

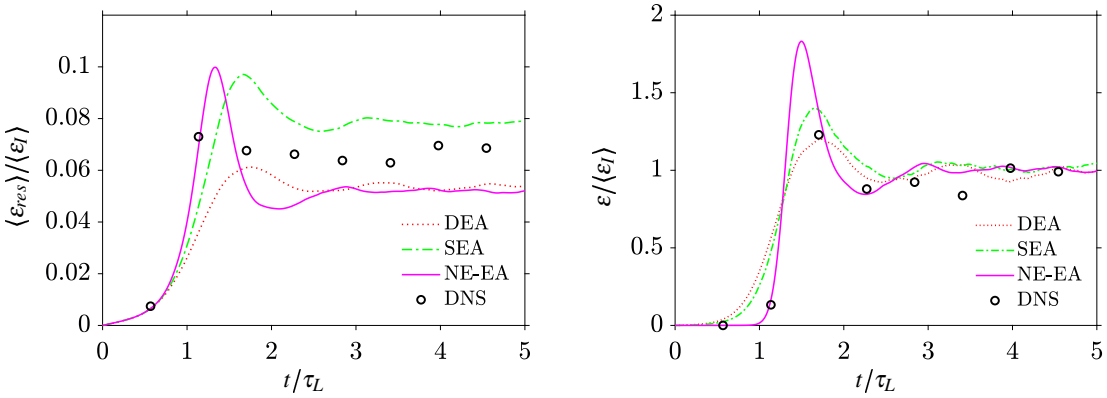

Figure 4: Evolution of the volume averaged dissipation in the resolved scales (left) and SGS kinetic energy dissipation (right).

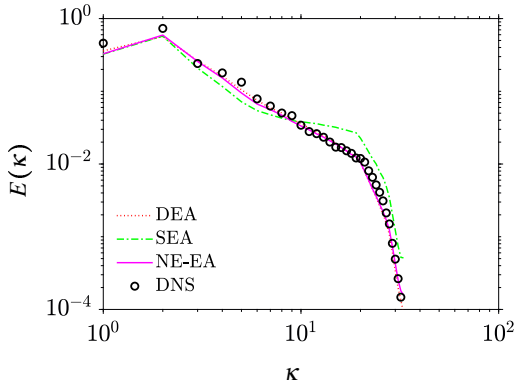

Figure 5: Averaged spectrum obtained of the different EASSMs generated using a homogeneous forcing scheme. The DNS data is filtered using a spectral cut-off filter with $\kappa_c = 20$.

(dynamic version). Our non-equilibrium model is denoted as NEA in the following.

The numerical method and the computational domain for DNS and LES are the same as described in the previous section. Only the numerical resolution has changed to adapt to the higher Re_λ: the DNS runs are performed with 1536^3 and the LES runs with 40^3 degrees of freedom, respectively. For comparison of DNS and LES, the results from the DNS are filtered with a three-dimensional explicit spectral cut-off filter ($\kappa_c = 20$).

All simulations are initialized with a flow at rest, i.e., $u_i(t = 0) = 0$, and the observed slow transition to a fully developed turbulent flow field is controlled by a large scale forcing (Alvelius, 1999) with energy input $\varepsilon_I = \text{const}$. In Fig. 3, we show $\langle k_{res}\rangle$ and $\langle k_{sgs}\rangle$ non-dimensionalised with their respective time averaged values at steady state, $\overline{\langle k_{res}\rangle}$ and $\overline{\langle k_{sgs}\rangle}$. Differently, the $\langle \varepsilon_{res}\rangle$ and the $\langle \varepsilon\rangle$ in Fig. 4 are non-dimensionalised using the box-averaged energy input rate due to the forcing, i.e., $\langle \varepsilon_I\rangle$. The time evolution of the quantities are plotted for $t = 5\tau_L$, where τ_L is the large eddy turnover time. The presence of a prominent peak in the evolution of the domain averaged quantities, both $\langle k_{res}\rangle/\overline{\langle k_{res}\rangle}$ and $\langle k_{sgs}\rangle/\overline{\langle k_{sgs}\rangle}$ are well captured by the NEA model. Furthermore, in the transient of $\langle k_{sgs}\rangle/\overline{\langle k_{sgs}\rangle}$, the DNS shows a delayed formation of the SGS scales in the simulation, i.e., they are formed only after about $t = 0.5\tau_L$. In LES, we see that only the NEA model captures this delay, while the DEA and the SEA models predict a growth of the k_{sgs} right from the start of the simulation. The ability of the NEA model to capture the correct transient of $\langle k_{sgs}\rangle/\overline{\langle k_{sgs}\rangle}$ is attributed to the additional model equation for the evolution of k_{sgs}. On the other hand, algebraic closures used to determine k_{sgs}, as in the SEA the DEA, imply an instantaneous adaptation of k_{sgs} to the resolved scales, as mentioned earlier. There-

fore, the SGS scales also start to develop instantaneously as soon as the forcing injects energy into the large and resolved scales. As a result, the delayed growth observed in DNS and with the NEA model is not captured by the SEA and the DEA models.

The evolution of $\langle \varepsilon_{res} \rangle / \langle \varepsilon_I \rangle$ and $\langle \varepsilon \rangle / \langle \varepsilon_I \rangle$ is shown in Fig. 4. The level of the mean resolved dissipation is also an indication of the energy density of the spectrum at higher wave numbers. Higher energy density at larger wave numbers correspond to a higher level of resolved dissipation. This will become more evident when we discuss the time averaged resolved energy spectrum in Fig. 5. From Fig. 4, it can be seen that in terms of the final steady state values, the NEA and the DEA give similar predictions of $\langle \varepsilon_{res} \rangle / \langle \varepsilon_I \rangle$. The SEA stands apart and over-predicts the level of the mean resolved dissipation as compared to the DEA, the NEA and the DNS. The peak in the evolution of $\langle \varepsilon_{res} \rangle / \langle \varepsilon_I \rangle$ is only captured by the NEA. This is also seen in the evolution of $\langle \varepsilon \rangle / \langle \varepsilon_I \rangle$, where only the NEA captures the slow initial growth and the peak. In this aspect, the proposed model is a clear improvement.

Finally, the time averaged three-dimensional energy spectrum for the statistically stationary state is shown in Fig. 5. Results for the DEA and NEA are very similar and both closely resemble the data from the DNS. As mentioned, this was already expected from the very similar resolved dissipation at statistical steady state. Not surprisingly, the SEA shows an accumulation of energy at higher wave numbers, which indicates insufficient accuracy of the energy dissipation from the resolved scales by the SEA.

REFERENCES

Alvelius, K. 1999 Random forcing of three-dimensional homogeneous turbulence. *Physics of Fluids* **11** (7), 1880–1889.

Germano, M. 1992 Turbulence: the filtering approach. *Journal of Fluid Mechanics* **238**, 325–336.

Germano, M., Piomelli, U., Moin, P. & Cabot, W. H. 1991 A dynamic subgrid-scale eddy viscosity model. *Physics of Fluids A: Fluid Dynamics* **3** (7), 1760–1765.

Girimaji, S. S. 1996 Fully explicit and self-consistent algebraic Reynolds stress model. *Theoretical and Computational Fluid Dynamics* **8** (6), 387–402.

Gnanasundaram, A. K., Pestana, T. & Hickel, S. 2019 A priori investigations into the construction and the performance of an explicit algebraic subgrid-scale stress model. In *Proceedings of 11th International Symposium on Turbulence and Shear Flow Phenomena (TSFP11)*.

Horiuti, K. 2003 Roles of non-aligned eigenvectors of strain-rate and subgrid-scale stress tensors in turbulence generation. *Journal of Fluid Mechanics* **491**, 65–100.

Launder, B. E., Reece, G. J. & Rodi, W. 1975 Progress in the development of a Reynolds-stress turbulence closure. *Journal of Fluid Mechanics* **68** (03), 537–566.

Lumley, J. L. & Newman, G. R. 1977 The return to isotropy of homogeneous turbulence. *Journal of Fluid Mechanics* **82** (1), 161–178.

Marstorp, L., Brethouwer, G., Grundestam, O. & Johansson, A. V. 2009 Explicit algebraic subgrid stress models with application to rotating channel flow. *Journal of Fluid Mechanics* **639**, 403–432.

Meneveau, C. & Katz, J. 2000 Scale-invariance and turbulence models for large-eddy simulation. *Annual Review of Fluid Mechanics* **32** (1), 1–32.

Montecchia, M., Brethouwer, G., Johansson, A. V. & Wallin, S. 2017 Taking large-eddy simulation of wall-bounded flows to higher Reynolds numbers by use of anisotropy-resolving subgrid models. *Physical Review Fluids* **2** (3), 034601.

Pestana, T. & Hickel, S. 2019 Regime transition in the energy cascade of rotating turbulence. *Physical Review E* **99** (5), 053103.

Pope, S. B. 1975 A more general effective-viscosity hypothesis. *Journal of Fluid Mechanics* **72** (02), 331–340.

Rodi, W. 1972 *The prediction of free turbulent boundary layers by use of a two-equation model of turbulence*. University of London.

Rotta, J. 1951 Statistische Theorie nichthomogener Turbulenz. *Z. Physik* **129**, 547–572.

Tao, B., Katz, J. & Meneveau, C. 2000 Geometry and scale relationships in high Reynolds number turbulence determined from three-dimensional holographic velocimetry. *Physics of Fluids* **12** (5), 941–944.

Taulbee, D. B. 1992 An improved algebraic Reynolds stress model and corresponding nonlinear stress model. *Physics of Fluids A: Fluid Dynamics* **4** (11), 2555–2561.

Wallin, S. & Johansson, A. V. 2000 An explicit algebraic Reynolds stress model for incompressible and compressible turbulent flows. *Journal of Fluid Mechanics* **403**, 89–132.

Wang, B. C. & Bergstrom, D. J. 2005 A dynamic nonlinear subgrid-scale stress model. *Physics of Fluids* **17** (3), 035109.

Yoshizawa, A. & Horiuti, K. 1985 A statistically-derived subgrid-scale kinetic energy model for the large-eddy simulation of turbulent flows. *Journal of the Physical Society of Japan* **54** (8), 2834–2839.